

Ion optics with electrostatic lenses

F. Hinterberger

Helmholtz-Institut für Strahlen- und Kernphysik, University of Bonn, Germany

Abstract

Ion optics with electrostatic lenses is presented using the standard matrix formalism of magnetic ion optics. We introduce the paraxial ray equation which is appropriate to systems with rotational symmetry. The first-order solutions of the paraxial ray equation are derived. The resulting transport matrices can be used to study systems with acceleration tube lenses, aperture lenses, einzel lenses and dc accelerators. The analogy with geometrical optics is discussed. Beam transport and phase ellipses are described using the so-called σ matrices. The equations of the longitudinal transport matrix are derived. Besides rotational symmetric elements, electrostatic quadrupoles and electrostatic deflectors are also presented. The effect of space charge forces is discussed.

1 Introduction

Electrostatic lenses are used for the extraction, preparation and first acceleration of electron and ion beams. Very often ion optics with electrostatic lenses is called electron optics. Electrostatic lenses are of great importance in the design of low energy electrostatic accelerators like Cockcroft–Walton and Van de Graaff accelerators. A broad field of application is the beam preparation of low energy electron and ion beams for scattering experiments. Even storage rings using solely electrostatic deflection and focusing devices have been developed. The theory of electrostatic lenses has been developed in the time 1930–1955. The solution of the paraxial ray equation and the introduction of the matrix formalism refers to the work of Gans [1], Elkind [2] and Timm [3]. The method is also reported by Galejs and Rose [4]. The solution of the paraxial ray equation at relativistic energies can be found in the books of Zworykin et al. [5] and Lawson [6]. Ion optics with rotational symmetric electrostatic lenses is presented in the book of Hinterberger [7]. Ion optics with transverse electric fields has been covered in the books of Banford [8], Dahl [9] and Wollnik [10]. Here, the first-order matrix formalism of ion optics with electrostatic lenses is presented following the book of Hinterberger [7]. At the end the effect of space charge forces is sketched.

2 Coordinate system and matrix formalism

We define a coordinate system as in magnetic ion optics [11–13], see Fig. 1. At any specified position s in the ion optical system an arbitrary charged particle is represented by a vector \vec{x} whose components specify the position, angle and relative momentum deviation with respect to a reference particle on a reference trajectory (central trajectory), i.e.,

$$\vec{x}(s) = \begin{pmatrix} x_1 \\ x_2 \\ x_3 \\ x_4 \\ x_5 \\ x_6 \end{pmatrix} = \begin{pmatrix} x \\ x' \\ y \\ y' \\ l \\ \delta \end{pmatrix} = \begin{pmatrix} \text{horizontal (radial) displacement} \\ \text{horizontal (radial) angle deviation} \\ \text{vertical (axial) displacement} \\ \text{vertical (axial) angle deviation} \\ \text{path length difference} \\ \text{relative momentum deviation} \end{pmatrix}. \quad (1)$$

This vector is referred to as ray. The curvilinear coordinate system with the unit vectors $(\vec{u}_x, \vec{u}_y, \vec{u}_s)$ moves with the arbitrary particle along the central trajectory, the arc length s specifies the distance from the origin along the central trajectory. When the reference trajectory is being deflected by an electrostatic

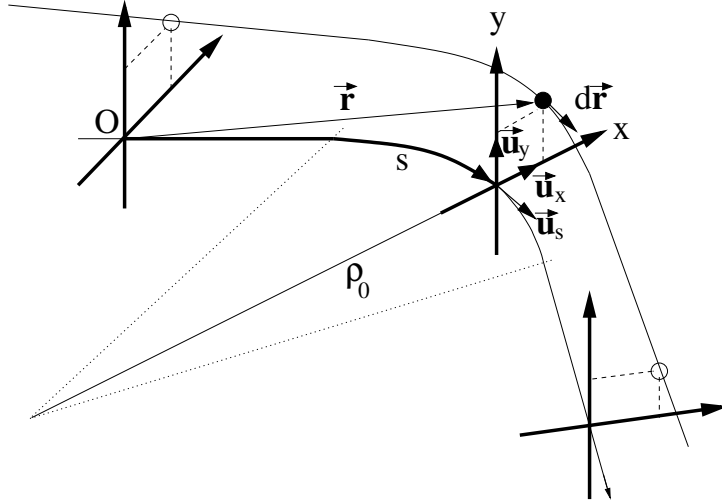


Fig. 1: Accompanying coordinate system [14]

deflector or a bending magnet or when electric or magnetic quadrupoles are being used, the direction of the vertical (axial) y -axis is chosen to be the normal to the electric or magnetic midplane. When only rotational symmetric electrostatic elements are being used, the azimuthal orientation of the (x, y) coordinate system can be freely chosen. The transformation of the ray coordinates by an ion optical system is represented to first order by a 6×6 matrix $R(s)$,

$$\vec{x}(s) = R(s)\vec{x}(0). \quad (2)$$

In a system with electric or magnetic midplane symmetry the transformation of the radial and axial coordinates are decoupled and the general form of the transport matrix R reads

$$R = \begin{pmatrix} R_{11} & R_{12} & 0 & 0 & 0 & R_{16} \\ R_{21} & R_{22} & 0 & 0 & 0 & R_{26} \\ 0 & 0 & R_{33} & R_{34} & 0 & 0 \\ 0 & 0 & R_{43} & R_{44} & 0 & 0 \\ R_{51} & R_{52} & 0 & 0 & R_{55} & R_{56} \\ 0 & 0 & 0 & 0 & 0 & R_{66} \end{pmatrix}. \quad (3)$$

In a system consisting only of rotational symmetric electrostatic lenses the matrix elements R_{16} , R_{26} , R_{51} and R_{52} are zero and the radial and axial submatrices are equal, i.e.,

$$R = \begin{pmatrix} R_{11} & R_{12} & 0 & 0 & 0 & 0 \\ R_{21} & R_{22} & 0 & 0 & 0 & 0 \\ 0 & 0 & R_{11} & R_{12} & 0 & 0 \\ 0 & 0 & R_{21} & R_{22} & 0 & 0 \\ 0 & 0 & 0 & 0 & R_{55} & R_{56} \\ 0 & 0 & 0 & 0 & 0 & R_{66} \end{pmatrix}, \quad (4)$$

$$\begin{pmatrix} x(s) \\ x'(s) \end{pmatrix} = \begin{pmatrix} R_{11} & R_{12} \\ R_{21} & R_{22} \end{pmatrix} \begin{pmatrix} x(0) \\ x'(0) \end{pmatrix}, \quad \begin{pmatrix} y(s) \\ y'(s) \end{pmatrix} = \begin{pmatrix} R_{11} & R_{12} \\ R_{21} & R_{22} \end{pmatrix} \begin{pmatrix} y(0) \\ y'(0) \end{pmatrix}. \quad (5)$$

Often, cylinder coordinates¹ (r, φ, s) are used in order to formulate the ion optics of cylinder symmetric electrostatic lenses. As a consequence, only meridional trajectories $r(s), r'(s)$ with $\varphi = \text{const}$ are evaluated and the properties of skewed rays (rays with $\varphi' \neq 0$) are not considered. This unnecessary restriction

¹The relation with Cartesian coordinates is given by $x = r \cos \varphi$, $y = r \sin \varphi$.

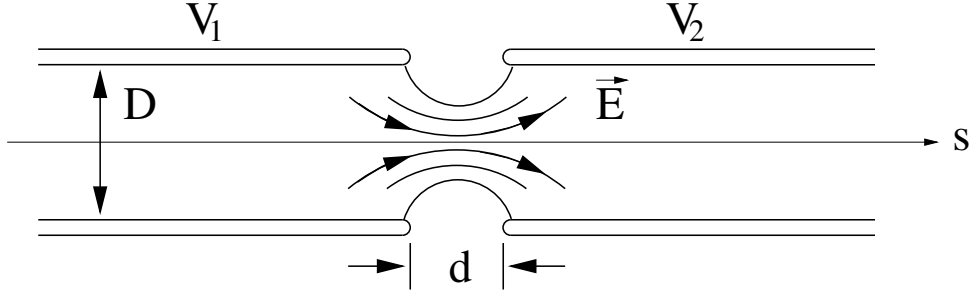


Fig. 2: Scheme of an accelerating tube lens [14]. The voltages V_1 and V_2 denote the potential differences with respect to the ion source. The electric field \vec{E} acts at the entrance of the accelerating gap as a focusing lens and at the exit as a defocusing lens.

is avoided by using Cartesian coordinates (x, x') and (y, y') instead of meridional ray coordinates (r, r') . In linear approximation the transport matrices for (r, r') and (x, x') or (y, y') are identical.

3 The paraxial ray equation

The central element of electrostatic ion optics is the accelerating tube lens (immersion lens). The accelerating tube lens consists of two metal tubes with different electrical potentials V_1 and V_2 as indicated in Fig. 2. We derive the paraxial ray equation for such rotational symmetric electric fields. The reader not interested in the derivation and first order solution of the paraxial ray equation may jump directly to Eq. (26) in Section 4.1. The starting point is Newton's equation of motion,

$$\frac{d}{dt} \vec{p} = q \vec{E} = q(-\vec{\nabla}V) . \quad (6)$$

With $\vec{E} = -\vec{\nabla}V$ the components may be written

$$\begin{aligned} \frac{d}{dt}(\gamma m \dot{x}) &= -q \frac{\partial V}{\partial x} , \\ \frac{d}{dt}(\gamma m \dot{y}) &= -q \frac{\partial V}{\partial y} , \\ \frac{d}{dt}(\gamma m \dot{s}) &= -q \frac{\partial V}{\partial s} . \end{aligned} \quad (7)$$

The equations of motion for x and y are equal due to the rotational symmetry, $(\partial V / \partial x = \partial V / \partial y)$. Therefore it is sufficient to consider the equation of motion for e.g., x . We replace the time t by the arc length s by introducing the component v_s of the momentary particle velocity in the direction of \vec{u}

$$v_s = \dot{s} = \frac{ds}{dt}, \quad \frac{d}{dt} = v_s \frac{d}{ds} . \quad (8)$$

In this context we note the equations

$$\dot{x} = v_s x', \quad \dot{y} = v_s y', \quad v^2 = v_s^2 (1 + x'^2 + y'^2) . \quad (9)$$

In a first step \dot{x} in Eq. (7) is replaced by $v_s x'$,

$$\frac{d}{dt}(\gamma m v_s x') = -q \frac{\partial V}{\partial x} .$$

yielding

$$x' \frac{d}{dt}(\gamma m v_s) + \gamma m v_s \frac{d}{dt} x' = -q \frac{\partial V}{\partial x} .$$

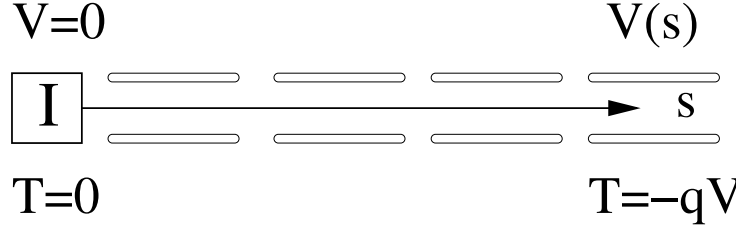


Fig. 3: Relation between the kinetic energy T and the electric potential V . I: ion source [14]

In a second step the first term is replaced according to Eq. (7) and the second term is modified according to Eq. (8),

$$x'(-q\frac{\partial V}{\partial s}) + \gamma mv_s^2 x'' = -q\frac{\partial V}{\partial x}.$$

Taking Eq. (9) into consideration we finally obtain the paraxial ray equation for x and similarly for y ,

$$\begin{aligned} x'' &= \frac{1+x'^2+y'^2}{\gamma mv^2} q \left(x' \frac{\partial V}{\partial s} - \frac{\partial V}{\partial x} \right), \\ y'' &= \frac{1+x'^2+y'^2}{\gamma mv^2} q \left(y' \frac{\partial V}{\partial s} - \frac{\partial V}{\partial y} \right). \end{aligned} \quad (10)$$

The quantity γmv^2 is equal to the product of velocity v and momentum p , $\gamma mv^2 = pv = p\beta c$. It defines the electric rigidity, $|\vec{E}|\rho = pv/q$ (see Section 8.2). The dependence on the kinetic energy T , the total energy E and the rest energy mc^2 reads

$$\gamma mv^2 = pv = \frac{(pc)^2}{E} = \frac{2mc^2T + T^2}{mc^2 + T} = T \frac{2mc^2 + T}{mc^2 + T}. \quad (11)$$

The kinetic energy T of a particle in the electric field is given by the momentary value of the electric potential $V(\vec{r})$. In the theory of electrostatic lenses the ion or electron source is chosen as zero point for the electric potential V (see Fig. 3). There, the kinetic energy T is also zero and the conservation of energy may be written

$$T + qV = 0, \quad T = -qV. \quad (12)$$

The electric charge q of electrons and negative ions is negative and the electric potential V must be positive in order to achieve acceleration. The electric charge of positive ions is positive and V must be negative. In both cases the quantity $-qV$ is positive and Eq. (11) may be written

$$\gamma mv^2 = pv = -qV \frac{2mc^2 - qV}{mc^2 - qV}. \quad (13)$$

The nonrelativistic approximation, that means $-qV \ll mc^2$, may be written

$$pv \approx 2T = -2qV. \quad (14)$$

Now we take the Laplace equation $\Delta V = 0$ and the rotational symmetry into account. Taking cylinder coordinates the potential distribution may be written

$$V(r, \varphi, s) = \sum_{n=0}^{\infty} (-1)^n \frac{V^{2n}}{(n!)^2} \left(\frac{r}{2} \right)^{2n}, \quad (15)$$

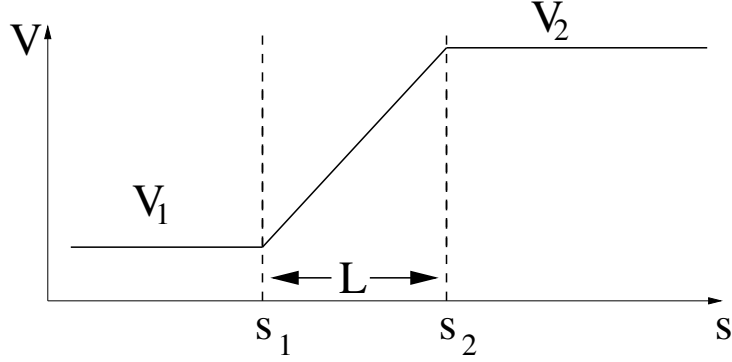


Fig. 4: Rough approximation of the potential $V(s)$ along the axis of an accelerating tube lens assuming particles with negative charge q . $L \approx D + d$ [14]

$$V(r, \varphi, s) = V(s) - \frac{r^2}{4} V''(s) + \dots \quad (16)$$

Taking Cartesian coordinates the potential may be written

$$V(x, y, s) = V(s) - \frac{x^2 + y^2}{4} V''(s) + \dots \quad (17)$$

The function $V(s)$ is the electric potential along the central trajectory. Knowing $V(s)$ allows to deduce the full potential distribution $V(x, y, s)$. In linear approximation we obtain

$$\begin{aligned} \frac{\partial V}{\partial x} &= -\frac{x}{2} V'', \\ \frac{\partial V}{\partial y} &= -\frac{y}{2} V''. \end{aligned}$$

In linear approximation the paraxial equation may be written (neglecting terms with x'^2 and y'^2)

$$\begin{aligned} x'' &= \frac{q}{pv} \left(x' V' + \frac{x}{2} V'' \right), \\ y'' &= \frac{q}{pv} \left(y' V' + \frac{y}{2} V'' \right). \end{aligned} \quad (18)$$

4 Solution of the paraxial ray equation

4.1 Rough approximation: single uniform field step

The potential distribution $V(s)$ along the symmetry axis is approximated by a linear rise between s_1 and s_2 as shown in Fig. 4. In order to avoid the sign problems discussed in the context of Eq. (12) we assume particles with negative charge like electrons and negative ions. The solution follows the work of Timm [3] and Zworykin et al. [5]. Due to the rotational symmetry it is sufficient to find the solution for the component in x direction. First we find the solution for the transition points at s_1 and s_2 .

At the transition points s_1 and s_2 the contribution of the term $x'V'$ to the integral is negligible. Therefore we consider only the effect of the term xV'' in Eq. (18). The integration yields

$$\Delta x' = \lim_{\Delta s \rightarrow 0} \int_{s_i - \Delta s}^{s_i + \Delta s} x'' ds = \lim_{\Delta s \rightarrow 0} \int_{s_i - \Delta s}^{s_i + \Delta s} \frac{xqV''}{2pv} ds, \quad i = 1, 2. \quad (19)$$

$$s_1 : \Delta x' = +\frac{q}{2p_1 v_1} \frac{V_2 - V_1}{L} x_1 = -\frac{1}{2p_1 v_1} \frac{T_2 - T_1}{L} x_1 = -\frac{1}{2p_1 v_1} \frac{E_2 - E_1}{L} x_1.$$

$$s_2 : \Delta x' = -\frac{q}{2p_2v_2} \frac{V_2 - V_1}{L} x_2 = +\frac{1}{2p_2v_2} \frac{T_2 - T_1}{L} x_2 = +\frac{1}{2p_2v_2} \frac{E_2 - E_1}{L} x_2 .$$

The resulting change $\Delta x'$ is negative (focusing) at s_1 and positive (defocusing) at s_2 . It is proportional to the momentary displacement $x_1 = x(s_1)$ and $x_2 = x(s_2)$, respectively and the potential gradient $V' = (V_2 - V_1)/L$, i.e., the energy gradient $E' = (E_2 - E_1)/L$ and inversely proportional to the momentary value of pv . The corresponding transport matrices (thin lens approximation) read

$$R_x(s_1) = \begin{pmatrix} 1 & 0 \\ -\frac{1}{2p_1v_1} \frac{E_2 - E_1}{L} & 1 \end{pmatrix}, \quad R_x(s_2) = \begin{pmatrix} 1 & 0 \\ +\frac{1}{2p_2v_2} \frac{E_2 - E_1}{L} & 1 \end{pmatrix} . \quad (20)$$

In the region between s_1 and s_2 $V'' = 0$ and Eq. (18) yields

$$\frac{x''}{x'} = \frac{qV'}{pv} = -\frac{\dot{p}}{pv} = -\frac{p'}{p}, \quad \ln x'_2 - \ln x'_1 = \ln p_1 - \ln p_2, \quad \frac{x'_2}{x'_1} = \frac{p_1}{p_2} .$$

The change of x is obtained by integration of $x' = x'_1 p_1 / p$,

$$x_2 - x_1 = \int_1^2 x' ds = x'_1 p_1 \int_1^2 \frac{ds}{p} . \quad (21)$$

The nonrelativistic solution is obtained by taking $p \sim \sqrt{V}$ and replacing ds by dV using $\frac{dV}{ds} = \frac{V_2 - V_1}{L} = const$,

$$\begin{aligned} x_2 - x_1 &= x'_1 \sqrt{V_1} \frac{L}{V_2 - V_1} \int_1^2 \frac{dV}{\sqrt{V}} \\ &= x'_1 \sqrt{V_1} \frac{L}{V_2 - V_1} 2(\sqrt{V_2} - \sqrt{V_1}) \\ &= x'_1 L \frac{2}{1 + \sqrt{V_2/V_1}} \\ &= x'_1 L \frac{2}{1 + p_2/p_1} . \end{aligned} \quad (22)$$

The complete matrix in nonrelativistic approximation reads with $N = T_2/T_1$

$$\begin{aligned} R_x &= \begin{pmatrix} 1 & 0 \\ +\frac{N-1}{4N} \frac{1}{L} & 1 \end{pmatrix} \begin{pmatrix} 1 & \frac{2}{1+\sqrt{N}} L \\ 0 & \frac{1}{\sqrt{N}} \end{pmatrix} \begin{pmatrix} 1 & 0 \\ -\frac{N-1}{4} \frac{1}{L} & 1 \end{pmatrix} \\ &= \begin{pmatrix} \frac{3-\sqrt{N}}{2} & \frac{2}{1+\sqrt{N}} L \\ -\frac{3}{8} \frac{(N-1)(\sqrt{N}-1)}{N} \frac{1}{L} & \frac{3\sqrt{N}-1}{2N} \end{pmatrix} . \end{aligned} \quad (23)$$

The relativistic exact solution is obtained replacing ds by dp using $\dot{p} = v \frac{dp}{ds} = -qV' = -q \frac{V_2 - V_1}{L} = \frac{E_2 - E_1}{L}$,

$$\begin{aligned} x_2 - x_1 &= x'_1 p_1 \frac{L}{E_2 - E_1} \int_1^2 v \frac{dp}{p} \\ &= x'_1 p_1 \frac{L}{E_2 - E_1} \int_1^2 \frac{c^2 dp}{\sqrt{(mc^2)^2 + (pc)^2}} \\ &= x'_1 L \frac{p_1 c}{E_2 - E_1} \ln \frac{p_2 c + E_2}{p_1 c + E_1} . \end{aligned} \quad (24)$$

Thus, the transport matrix for a region with constant energy gradient reads

$$R_x = \begin{pmatrix} 1 & L_{\text{eff}} \\ 0 & p_1/p_2 \end{pmatrix}, \quad L_{\text{eff}} = L \frac{p_1 c}{E_2 - E_1} \ln \frac{p_2 c + E_2}{p_1 c + E_1} . \quad (25)$$

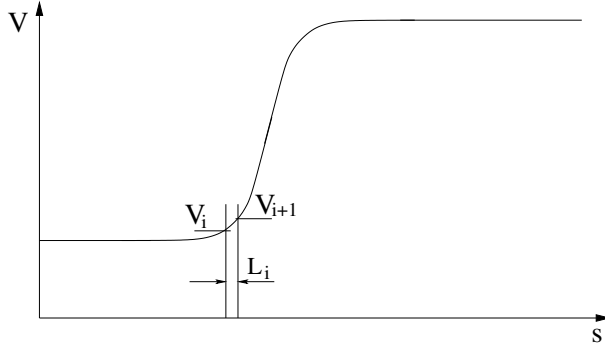


Fig. 5: Subdivision into n segments [14]

The relativistic exact complete matrix including the transitions at s_1 and s_2 reads

$$R_x = \begin{pmatrix} 1 & 0 \\ +\frac{E_2-E_1}{2p_2v_2} \frac{1}{L} & 1 \end{pmatrix} \begin{pmatrix} 1 & L_{\text{eff}} \\ 0 & \frac{p_1}{p_2} \end{pmatrix} \begin{pmatrix} 1 & 0 \\ -\frac{E_2-E_1}{2p_1v_1} \frac{1}{L} & 1 \end{pmatrix}. \quad (26)$$

The complete matrix is the product of three matrices. For $E_2 > E_1$ we have the sequence

focusing lens – modified drift – defocusing lens.

For $E_2 < E_1$ we have the opposite sequence. In both cases the focusing is stronger than the defocusing. The determinant reads

$$\det(R_x) = p_1/p_2. \quad (27)$$

4.2 Refined treatment: segmentation

The ion optical determination of an accelerating tube lens can be refined by subdividing the whole assembly in many short segments (see Fig. 5) and by representing the potential distribution $V(s)$ in the form of a polygon. This method was invented by Timm [3]. It allows a more precise representation of the axial potential $V(s)$. We note the matrix $R_i = R_{x,i} = R_{y,i}$ of a single segment which has the same structure as Eq. (26),

$$R_i = \begin{pmatrix} 1 & 0 \\ +\frac{E_{i+1}-E_i}{2p_{i+1}v_{i+1}} \frac{1}{L_i} & 1 \end{pmatrix} \begin{pmatrix} 1 & L_{\text{eff},i} \\ 0 & \frac{p_i}{p_{i+1}} \end{pmatrix} \begin{pmatrix} 1 & 0 \\ -\frac{E_{i+1}-E_i}{2p_iv_i} \frac{1}{L_i} & 1 \end{pmatrix}. \quad (28)$$

The length L_i of the individual segments can be chosen freely. In a region with a large curvature of the function $V(s)$, i.e., where V'' is large, very short segments are appropriate. The complete transport matrix of n segments is given as matrix product

$$R = R_n R_{n-1} \cdots R_1. \quad (29)$$

The matrix R represents R_x and R_y , $R = R_x = R_y$.

The function $V(s)$ can be determined experimentally or by numerical solution of the Laplace equation $\Delta V = 0$. For many applications analytical approximations are sufficient. For instance for two tubes with equal inner diameter D and a gap width d which is small with respect to D the analytic approximation [15] yields

$$V(s) = \frac{V_1 + V_2}{2} + \frac{V_1 - V_2}{2} \tanh \left(2, 64 \frac{s}{D} \right). \quad (30)$$

Here, we have $s = 0$ at the symmetry point between the two electrodes.

5 Elements of electrostatic ion optics

In this section we summarize the transport matrices of rotational symmetric electrostatic lenses.

5.1 Drift

The characteristic feature of a drift is the constancy of the potential $V(s)$, i.e., $V'(s) = 0$ und $V''(s) = 0$. For a drift of length L the transport matrix reads

$$R_x = R_y = \begin{pmatrix} 1 & L \\ 0 & 1 \end{pmatrix}. \quad (31)$$

5.2 Accelerating field

For a section with constant accelerating field we note

$$R_x = R_y = \begin{pmatrix} 1 & L_{\text{eff}} \\ 0 & p_1/p_2 \end{pmatrix}, \quad L_{\text{eff}} = L \frac{p_1 c}{E_2 - E_1} \ln \frac{p_2 c + E_2}{p_1 c + E_1}. \quad (32)$$

The subscripts 1 and 2 refer to the entrance and exit of the section. The formula can be applied for acceleration ($E_2 > E_1$) as well as deceleration ($E_2 < E_1$).

5.3 Aperture lens

A very simple and important lens is the so-called aperture lens. An aperture lens consists of a small circular hole in a conducting metal plate separating two regions with different longitudinal electric fields (see Fig. 6). A charged particle beam passing the aperture sees a focusing effect due to the sudden change of the voltage gradient. The transport matrix can be deduced using Eq. (19). Taking the difference of the energy gradients $E'_2 - E'_1$ the matrix reads

$$R_x = R_y = \begin{pmatrix} 1 & 0 \\ -(E'_2 - E'_1)/(2pv) & 1 \end{pmatrix}. \quad (33)$$

It is the matrix of a thin lens with the focusing power

$$\frac{1}{f} = \frac{E'_2 - E'_1}{2pv}. \quad (34)$$

The lens is focusing for $E'_2 > E'_1$ and defocusing for $E'_2 < E'_1$. The ion optics before and after the aperture lens is represented by matrices of the type accelerating field.

Applying Timm's method of subdividing a continuous potential distribution $V(s)$ in many small segments two matrices of the form of Eq. (20) are multiplied at the transition from segment $i - 1$ to segment i yielding with

$$E'_i - E'_{i-1} = \frac{E_{i+1} - E_i}{L_i} - \frac{E_i - E_{i-1}}{L_{i-1}} :$$

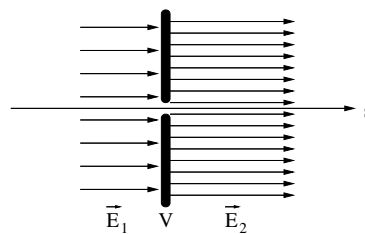
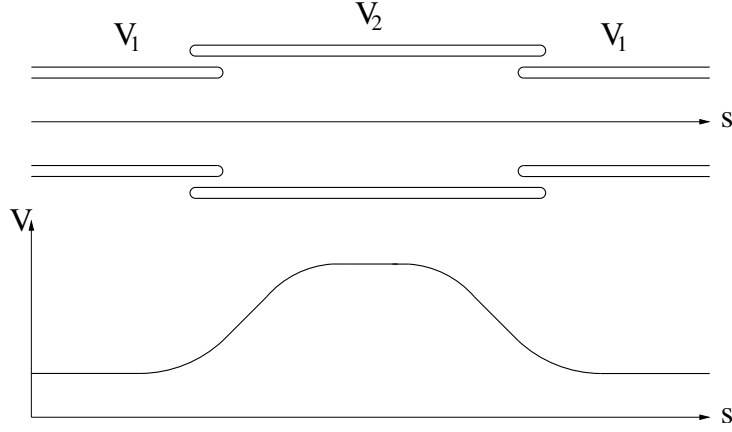


Fig. 6: Scheme of an aperture lens [14]

**Fig. 7:** Scheme of an einzel lens [14]

$$R_x = R_y = \begin{pmatrix} 1 & 0 \\ -\frac{E'_i - E'_{i-1}}{2p_i v_i} & 1 \end{pmatrix}. \quad (35)$$

The resulting matrix has the same form as the matrix of an aperture lens. Thus, one can always use the matrix of an aperture lens at a transition point with $E'_i \neq E'_{i-1}$ instead of multiplying a matrix for the transition $E'_{i-1} \rightarrow 0$ with a matrix for the transition $0 \rightarrow E'_i$.

5.4 Einzel lens

The einzel lens is a combination of the accelerating tube lenses with opposite polarity (see Fig. 7). This lens system has the property of a thick focusing lens for $V_2 > V_1$ as well as for $V_2 < V_1$. Passing an einzel lens does not change the energy of the charged particles. The complete transport matrix can be written as the product of two accelerating tube lenses

$$R = R(V_1, V_2)R(V_2, V_1). \quad (36)$$

The two matrices are evaluated using the rough approximation of Eq. (26) or the more elaborated approach of Eq. (29). It is also possible to subdivide the einzel lens in n segments and to apply immediately Eq. (29).

6 The transformation of the longitudinal coordinates

In this section we consider the transformation of the longitudinal coordinates (l, δ) in systems with rotational symmetric electrostatic acceleration fields. The knowledge of the longitudinal transport matrix is especially important for the beam preparation of pulsed beams if a high time of flight resolution is wanted. Often dc accelerators are used as preaccelerators. Then a proper matching of the pulsed beam onto the acceptance of a subsequent rf accelerator is of great importance.

For a *drift space* of length L the longitudinal transfer matrix reads like in magnetic ion optics

$$R_l = \begin{pmatrix} R_{55} & R_{56} \\ R_{65} & R_{66} \end{pmatrix} = \begin{pmatrix} 1 & L/\gamma^2 \\ 0 & 1 \end{pmatrix}. \quad (37)$$

In systems with electrostatic acceleration the energy deviation $\Delta E = E - E_0$ between a particle and the reference particle stays constant during the passage of an electrostatic accelerating field. Similarly the time difference $\Delta t = t - t_0$ between monoenergetic particles stays constant. But the longitudinal

coordinates (l, δ) are changed. The matrix element $R_{55} = (l|l_0)$ reads

$$R_{55} = \frac{v_2}{v_1}.$$

This equation is a consequence of the fact that the longitudinal distance between two particles changes if the velocity of the particles is changed (compare with a similar situation in the traffic). The matrix element $R_{65} = (\delta|l_0)$ is zero. We note

$$R_{65} = 0.$$

The matrix element $R_{66} = (\delta|\delta_0)$ can be deduced using the relativistic relation between velocity v , momentum p and total energy E . Differentiating $E^2 = p^2 + m^2$ yields $\Delta E = (p/E)\Delta p = v\Delta p$. Since the energy deviation stays constant, i.e., $\Delta E_2 = \Delta E_1$ we find

$$\frac{\Delta p_2}{\Delta p_1} = \frac{E_2}{p_2} \frac{p_1}{E_1} = \frac{v_1}{v_2}$$

and

$$R_{66} = \frac{\Delta p_2}{p_2} \frac{p_1}{\Delta p_1} = \frac{p_1 v_1}{p_2 v_2}.$$

The matrix element $R_{56} = (l|\delta_0)$ is deduced assuming a constant energy gradient $dE/ds = (E_2 - E_1)/L = \text{const}$,

$$\begin{aligned} R_{56} &= \int_1^2 \frac{v}{v_1} \frac{p_1 v_1}{p v} \frac{ds}{\gamma^2} = \frac{p_1}{\text{const}} \int_1^2 \frac{dE}{\gamma^2 p} \\ &= \frac{p_1 c}{\text{const}} \int_1^2 \frac{d\gamma}{\gamma^2 \sqrt{\gamma^2 - 1}} = \frac{p_1 c}{\text{const}} \frac{\sqrt{\gamma^2 - 1}}{\gamma} \Big|_1^2 = p_1 \frac{v_2 - v_1}{E_2 - E_1} L. \end{aligned}$$

Here, the term v/v_1 under the integral takes the change of the longitudinal distance into account. The term $(p_1 v_1)/(p v)$ takes the change of the relative momentum deviation into account. The term ds/γ^2 takes the change of the longitudinal distance due to the momentary velocity deviation $\Delta v/v = (1/\gamma^2)\delta$ into account. As discussed in Section 4.2 the full system can always be subdivided into smaller segments such that the assumption of a constant energy gradient is justified.

The complete longitudinal transport matrix R_l for an accelerating field with constant energy gradient reads

$$R_l = \begin{pmatrix} R_{55} & R_{56} \\ R_{65} & R_{66} \end{pmatrix} = \begin{pmatrix} \frac{v_2}{v_1} & p_1 \frac{v_2 - v_1}{E_2 - E_1} L \\ 0 & \frac{p_1 v_1}{p_2 v_2} \end{pmatrix}. \quad (38)$$

This equation holds for accelerating as well as decelerating fields. The determinant of R_l is equal to the ratio p_1/p_2 . For a negligibly small acceleration ($v_2 - v_1 \rightarrow 0$)

$$R_{56} \rightarrow \frac{1}{\gamma^2} L$$

and the longitudinal transport matrix has the form of Eq. (37).

For completeness we note R_l of an aperture lens,

$$R_l = \begin{pmatrix} R_{55} & R_{56} \\ R_{65} & R_{66} \end{pmatrix} = \begin{pmatrix} 1 & 0 \\ 0 & 1 \end{pmatrix}. \quad (39)$$

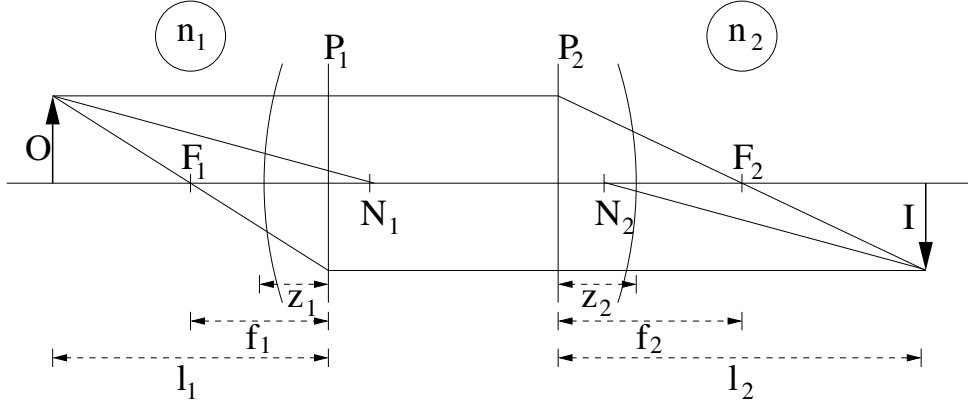


Fig. 8: Position of the cardinal planes of an accelerating tube lens with $n_2 > n_1$ [14]

7 Geometric optics

7.1 Focal length, principal planes and index of refraction

Applying the formalism of geometric optics the accelerating tube lens can be described as a thick focusing lens, see Fig. 8. Like in magnetic ion optics the focal lengths f_1 and f_2 and the position of the principal planes P_1 and P_2 can be deduced from the matrix elements of the transverse transport submatrix $R_x = R_y$. We note that the index of refraction² changes if particles are accelerated. For an accelerating tube lens the ratio of the indices of refraction reads

$$n = \frac{n_2}{n_1} = \frac{p_2}{p_1} . \quad (40)$$

As a consequence the focal lengths of the object and image planes are different. The ratio reads

$$\frac{f_2}{f_1} = \frac{n_2}{n_1} = n . \quad (41)$$

The transport submatrix $R_x = R_y$ of the accelerating tube lens may be written

$$R_x = \begin{pmatrix} R_{11} & R_{12} \\ R_{21} & R_{22} \end{pmatrix} = \begin{pmatrix} 1 & z_2 \\ 0 & 1 \end{pmatrix} \begin{pmatrix} 1 & 0 \\ -1/(f_2) & 1/n \end{pmatrix} \begin{pmatrix} 1 & z_1 \\ 0 & 1 \end{pmatrix} , \quad (42)$$

$$R_x = \begin{pmatrix} R_{11} & R_{12} \\ R_{21} & R_{22} \end{pmatrix} = \begin{pmatrix} 1 - \frac{z_2}{f_2} & z_1 + \frac{z_2}{n} - \frac{z_1 z_2}{f_2} \\ -\frac{1}{f_2} & \frac{1}{n} - \frac{z_1}{f_2} \end{pmatrix} . \quad (43)$$

This equation allows to deduce the positions z_1 and z_2 of the principal planes P_1 and P_2 with respect to the beginning and end of the accelerating tube lens as well as the focal lengths f_1 and $f_2 = n f_1$,

$$z_1 = \frac{R_{22} - \det(R_x)}{R_{21}} , \quad z_2 = \frac{R_{11} - 1}{R_{21}} , \quad f_1 = -\frac{\det(R_x)}{R_{21}} , \quad f_2 = -\frac{1}{R_{21}} . \quad (44)$$

The position of the so-called nodal planes N_1 and N_2 is also defined,

$$\overline{F_1 N_1} = f_2 , \quad \overline{N_2 F_2} = f_1 . \quad (45)$$

In this context we recall the special form of the condition for a point-to-point imaging

$$\frac{f_1}{l_1} + \frac{f_2}{l_2} = 1 . \quad (46)$$

²The change of the index of refraction n is the reason that an accelerating tube lens is called immersion lens.

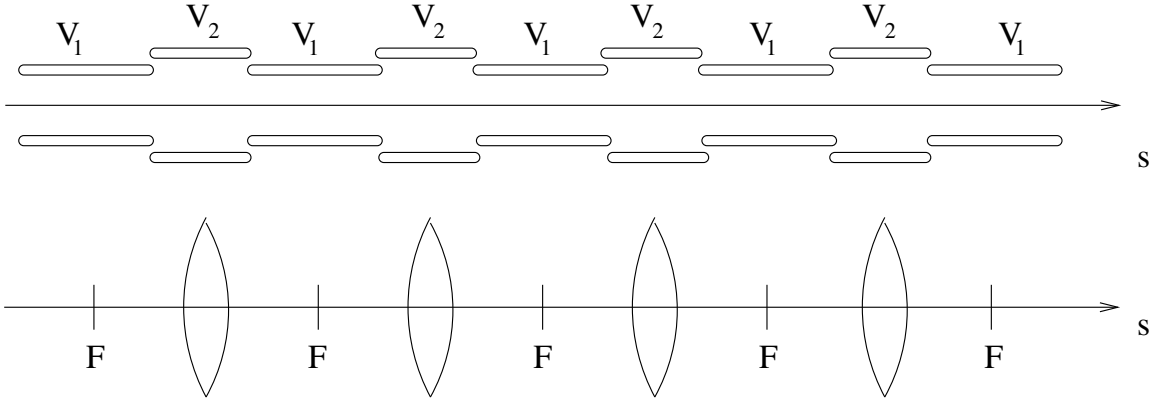


Fig. 9: Telescopic system of four einzel lenses and optical analogon [14]

Here, l_1 is the distance between the object plane and principal plane P_1 and l_2 the distance between image plane and principal plane P_2 . The lateral magnification M reads

$$M = -\frac{l_2 - f_2}{f_2} = -\frac{f_1}{l_1 - f_1} = -\frac{l_2 f_1}{l_1 f_2}. \quad (47)$$

7.2 Telescopic systems

A telescopic system consists of two focusing lenses where the second focal plane of the first lens coincides with the first focal plane of the second lens. The properties of telescopic systems can be studied using the matrix formalism. The transport matrix between the first and second focal plane of a thick focusing lens with focal length f may be written

$$R_{x,y} = \begin{pmatrix} 1 & f \\ 0 & 1 \end{pmatrix} \begin{pmatrix} 1 & 0 \\ -1/f & 1 \end{pmatrix} \begin{pmatrix} 1 & f \\ 0 & 1 \end{pmatrix} = \begin{pmatrix} 0 & f \\ -\frac{1}{f} & 0 \end{pmatrix}. \quad (48)$$

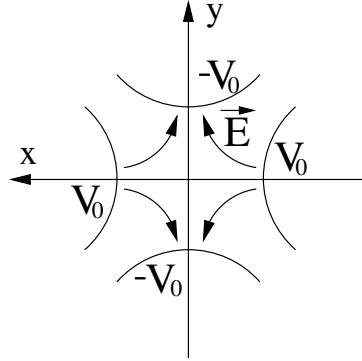
The telescopic combination of two identical focusing lenses yields a -1 telescope, i.e., a unit transformation with a minus sign,

$$R_{x,y} = \begin{pmatrix} 0 & f \\ -1/f & 0 \end{pmatrix} \begin{pmatrix} 0 & f \\ -1/f & 0 \end{pmatrix} = \begin{pmatrix} -1 & 0 \\ 0 & -1 \end{pmatrix}. \quad (49)$$

The combination of two telescopic systems yields again a telescopic system. Telescopic systems provide many advantages. With a telescopic system a simultaneous point-to-point and parallel-to-parallel imaging is possible. A point-to-point imaging provides automatically a waist-to-waist transformation. The combination of telescopic systems yields systems with favourable optical properties. For instance combining two identical -1 telescopes yields a $+1$ telescope where all geometric and many chromatic second-order aberrations vanish due to the inherent symmetry of the system [16–18]. Using einzel lenses telescopic systems can easily be realized. For example a -1 telescope can be built with two identical einzel lenses and a $+1$ telescope with four identical einzel lenses (see Fig. 9). Due to the rotational symmetry such systems are telescopic in both planes, i.e., double telescopic. Using one power supply for the voltage of the middle electrodes one has the benefit of a one knob control.

8 Electrostatic lenses with midplane symmetry

For completeness we list the first-order transport matrices of electrostatic elements with midplane symmetry. The formulas are presented following the derivations in the book of Banford [8].

**Fig. 10:** Electrostatic quadrupole

8.1 Electrostatic quadrupoles

The scheme of an electrostatic quadrupole is shown in Fig. 10.

Depending on the polarity of the electric fields the electrostatic quadrupole is focusing (defocusing) in the x direction and defocusing (focusing) in the y direction. The first-order transport matrix of a horizontally (radially) focusing and vertically (axially) defocusing electrostatic quadrupole reads

$$R = \begin{pmatrix} \cos \sqrt{k}L & \frac{\sin \sqrt{k}L}{\sqrt{k}} & 0 & 0 & 0 & 0 \\ -\sqrt{k} \sin \sqrt{k}L & \cos \sqrt{k}L & 0 & 0 & 0 & 0 \\ 0 & 0 & \cosh \sqrt{k}L & \frac{\sinh \sqrt{k}L}{\sqrt{k}} & 0 & 0 \\ 0 & 0 & \sqrt{k} \sinh \sqrt{k}L & \cosh \sqrt{k}L & 0 & 0 \\ 0 & 0 & 0 & 0 & 1 & L/\gamma^2 \\ 0 & 0 & 0 & 0 & 0 & 1 \end{pmatrix}. \quad (50)$$

Here, L is the effective length and k is given by the absolute value of the electric field gradient $|g| = |\vec{E}_0|/a = 2|V_0|/a^2$ at the pole tip and the electric rigidity $(E\rho)_0 = (pv)_0/q$ of the reference particle,

$$k = \frac{|g|}{(E\rho)_0} = \frac{2|V_0|}{a^2} \frac{1}{(E\rho)_0}. \quad (51)$$

Here, a is the radial distance of the pole tip from the axis and $|V_0|$ denotes the absolute value of the electric voltage at the pole tip. For a horizontally (radially) defocusing and vertically (axially) focusing electrostatic quadrupole the submatrices R_x and R_y are interchanged. The longitudinal submatrix R_l reads like for a drift space.

8.2 Electrostatic deflectors

The scheme of an electrostatic deflector is shown in Fig. 11. We assume the horizontal (radial) plane as the bending plane. An electrostatic deflector with toroidal electrodes provides focusing in x and y

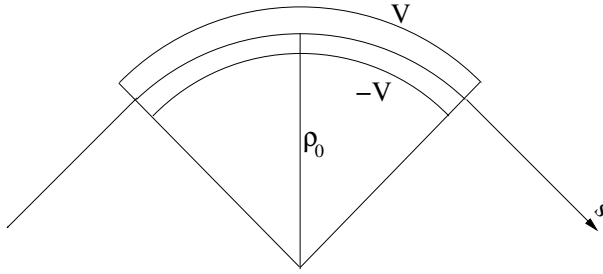


Fig. 11: Electrostatic deflector

direction and dispersion in the x and l direction. The first-order transport matrix reads

$$R = \begin{pmatrix} \cos \sqrt{k_x}L & \frac{\sin \sqrt{k_x}L}{\sqrt{k_x}} & 0 & 0 & 0 & \frac{2-\beta_0^2}{\rho_0 k_x} (1 - \cos \sqrt{k_x}L) \\ -\sqrt{k_x} \sin \sqrt{k_x}L & \cos \sqrt{k_x}L & 0 & 0 & 0 & \frac{2-\beta_0^2}{\rho_0 \sqrt{k_x}} \sin \sqrt{k_x}L \\ 0 & 0 & \cos \sqrt{k_y}L & \frac{\sin \sqrt{k_y}L}{\sqrt{k_y}} & 0 & 0 \\ 0 & 0 & -\sqrt{k_y} \sin \sqrt{k_y}L & \cos \sqrt{k_y}L & 0 & 0 \\ -\frac{\sin \sqrt{k_x}L}{\rho_0 \sqrt{k_x}} & \frac{\cos(\sqrt{k_x}L)-1}{\rho_0 k_x} & 0 & 0 & 1 & \frac{L}{\gamma^2} - \frac{2-\beta_0^2}{\rho_0^2 k_x} \left(L - \frac{\sin \sqrt{k_x}L}{\sqrt{k_x}} \right) \\ 0 & 0 & 0 & 0 & 0 & 1 \end{pmatrix} \quad (52)$$

Here, k_x and k_y depend on the bending radius $\rho_0 = (E\rho)_0/E_0$ of the reference particle, the velocity of the reference particle $\beta_0 = v_0/c$ and the electric field index $n_E = -(\rho_0/E_0)\partial E_x/\partial x$ with $(E\rho)_0$ the electric rigidity of the reference particle, E_0 the radial field on the reference orbit and $\partial E_x/\partial x$ its radial derivative. The effective length L is related to the bending angle α , $L = \rho_0 \alpha$. The field index n_E depends on the ratio of the horizontal (radial) ρ_0 and vertical (axial) r_0 radii of curvature of the midequipotential surface,

$$n_E = 1 + \frac{\rho_0}{r_0}, \quad k_x = \frac{3 - n_E - \beta_0^2}{\rho_0^2}, \quad k_y = \frac{n_E - 1}{\rho_0^2}. \quad (53)$$

From this equation we see that there is simultaneous focusing in the x and y directions provided that $1 < n_E < 3 - \beta_0^2$ which compares with $0 < n < 1$ for a bending magnet. A negative value of k_x or k_y yields defocusing in the x or y direction. If e.g., k_y is negative one has $\cos(\sqrt{k_y}L) = \cosh(\sqrt{|k_y|}L)$, $\sqrt{k_y} \sin(\sqrt{k_y}L) = -\sqrt{|k_y|} \sinh(\sqrt{|k_y|}L)$ and $\sin(\sqrt{k_y}L)/\sqrt{k_y} = \sinh(\sqrt{|k_y|}L)/\sqrt{|k_y|}$. For non-relativistic particles ($\beta_0 \approx 0$) a spherical electrostatic deflector with $r_0 = \rho_0$ yields equal horizontal (radial) and vertical (axial) focusing strengths, i.e., $k_x = k_y$. For an electrostatic deflector with cylindrical electrodes ($r_0 \rightarrow \infty$) the vertical (axial) submatrix R_y is the matrix of a drift space of length L .

9 Phase ellipses

The transverse phase ellipses are defined like in magnetic ion optics. They represent the properties of a beam. In rotational symmetric electrostatic systems the beam can be rotational symmetric, i.e., the phase ellipses for x, x' and y, y' are equal. But the formalism allows also to describe beams which are not rotational symmetric. The transverse and longitudinal phase ellipses are represented by the symmetric matrices σ_x , σ_y and σ_l ,

$$\begin{aligned} \sigma_x &= \begin{pmatrix} \sigma_{11} & \sigma_{12} \\ \sigma_{12} & \sigma_{22} \end{pmatrix}, \\ \sigma_y &= \begin{pmatrix} \sigma_{33} & \sigma_{34} \\ \sigma_{34} & \sigma_{44} \end{pmatrix}, \end{aligned} \quad (54)$$

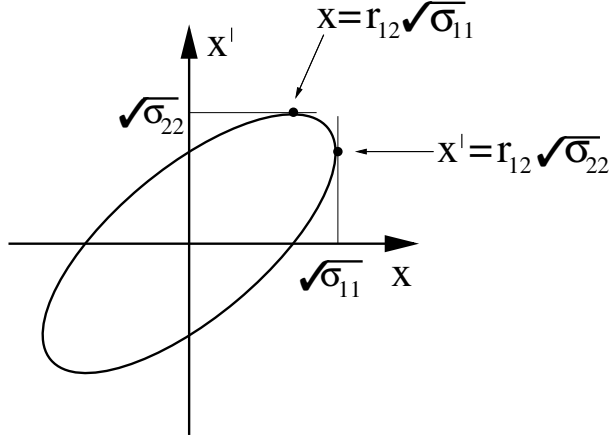


Fig. 12: Phase ellipse

$$\sigma_l = \begin{pmatrix} \sigma_{55} & \sigma_{56} \\ \sigma_{56} & \sigma_{66} \end{pmatrix}.$$

The equation of e.g., the horizontal phase ellipse may be written

$$(x, x') \sigma^{-1} \begin{pmatrix} x \\ x' \end{pmatrix} = 1. \quad (55)$$

yielding

$$\sigma_{22} x^2 - 2\sigma_{12} x x' + \sigma_{11} x'^2 = \det(\sigma_x) = \epsilon_x^2. \quad (56)$$

Here, (x, x') is the vector describing the contour of the phase ellipse (see Fig. 12). The emittance, i.e., the area of the ellipse, is given by

$$E_x = \pi \epsilon_x = \pi \sqrt{\sigma_{11} \sigma_{22} - \sigma_{12}^2}. \quad (57)$$

The maximum displacement in x and x' direction is given by

$$x_{max} = \sqrt{\sigma_{11}}, \quad x'_{max} = \sqrt{\sigma_{22}}. \quad (58)$$

Often, these values are defined as one, two or three standard deviations of the beam density distribution in x and x' direction. The matrix element σ_{12} is a measure of the correlation between x and x' . The correlation parameter r_{12} reads

$$r_{12} = \frac{\sigma_{12}}{\sqrt{\sigma_{11} \sigma_{22}}}. \quad (59)$$

The area and the shape of the phase ellipses represent the properties of a particle beam. If the density distributions of the beam are Gaussian the density distribution $\rho(\vec{x})$ in a phase space plane can be described by a normalized two-dimensional Gaussian distribution, e.g., with $\vec{x} = (x, x')$

$$\rho(\vec{x}) = \frac{1}{2\pi\epsilon_x} \exp\left(-\frac{1}{2}\vec{x}^T \sigma_x^{-1} \vec{x}\right). \quad (60)$$

The transformation of the phase ellipse by the ion optical system reads

$$\begin{aligned} \sigma_x(s) &= R_x(s) \sigma_x(0) R_x^T(s), \\ \sigma_y(s) &= R_y(s) \sigma_y(0) R_y^T(s), \end{aligned} \quad (61)$$

$$\sigma_l(s) = R_l(s)\sigma_l(0)R_l^T(s).$$

This allows to deduce the beam envelopes

$$\begin{aligned} x_{\max}(s) &= \sqrt{\sigma_{11}(s)}, \\ y_{\max}(s) &= \sqrt{\sigma_{33}(s)}, \\ l_{\max}(s) &= \sqrt{\sigma_{55}(s)}. \end{aligned} \quad (62)$$

Electrostatic acceleration tubes change the transverse and longitudinal beam emittances $\pi\epsilon_x$, $\pi\epsilon_y$ and $\pi\epsilon_l$,

$$\begin{aligned} \epsilon_x(s) &= \frac{p(0)}{p(s)}\epsilon_x(0), \\ \epsilon_y(s) &= \frac{p(0)}{p(s)}\epsilon_y(0), \\ \epsilon_l(s) &= \frac{p(0)}{p(s)}\epsilon_l(0). \end{aligned} \quad (63)$$

The emittances are inversely proportional to the beam momentum. This effect is called adiabatic damping.

The phase ellipse formalism may be extended to the six-dimensional phase space by defining a phase ellipsoid [11],

$$\vec{x}^T \sigma^{-1} \vec{x} = 1. \quad (64)$$

Here, σ is a symmetric 6×6 matrix with positive determinant and \vec{x} describes the contour of the ellipsoid. The matrices σ_x , σ_y and σ_l are submatrices of σ . For systems with midplane symmetry and beams with no correlation between the x, x' and y, y' subspaces the matrix σ reads

$$\sigma = \begin{pmatrix} \sigma_{11} & \sigma_{12} & 0 & 0 & \sigma_{15} & \sigma_{16} \\ \sigma_{12} & \sigma_{22} & 0 & 0 & \sigma_{25} & \sigma_{26} \\ 0 & 0 & \sigma_{33} & \sigma_{34} & 0 & 0 \\ 0 & 0 & \sigma_{34} & \sigma_{44} & 0 & 0 \\ \sigma_{15} & \sigma_{25} & 0 & 0 & \sigma_{55} & \sigma_{56} \\ \sigma_{16} & \sigma_{26} & 0 & 0 & \sigma_{56} & \sigma_{66} \end{pmatrix}. \quad (65)$$

The most general σ matrix including all possible covariances reads

$$\sigma = \begin{pmatrix} \sigma_{11} & \sigma_{12} & \sigma_{13} & \sigma_{14} & \sigma_{15} & \sigma_{16} \\ \sigma_{12} & \sigma_{22} & \sigma_{23} & \sigma_{24} & \sigma_{25} & \sigma_{26} \\ \sigma_{13} & \sigma_{23} & \sigma_{33} & \sigma_{34} & \sigma_{35} & \sigma_{36} \\ \sigma_{14} & \sigma_{24} & \sigma_{34} & \sigma_{44} & \sigma_{45} & \sigma_{46} \\ \sigma_{15} & \sigma_{25} & \sigma_{35} & \sigma_{45} & \sigma_{55} & \sigma_{56} \\ \sigma_{16} & \sigma_{26} & \sigma_{36} & \sigma_{46} & \sigma_{56} & \sigma_{66} \end{pmatrix}. \quad (66)$$

10 Space charge forces

If high-current beams are transported at low kinetic energies the space charge forces must be taken into account [13, 19, 20]. The primary effect of space charge forces is defocusing. But the nonlinear components of the space charge forces lead also to a slow increase in emittance. The defocusing effect of space charge forces can be simulated by adding a series of thin defocusing lenses. The example in Fig. 13 is shown in order to demonstrate (i) the defocusing effect due to space charge forces and (ii) the focusing effect of an accelerating tube. The first-order ion optical calculations have been performed using the PSI Graphic Transport program [13].

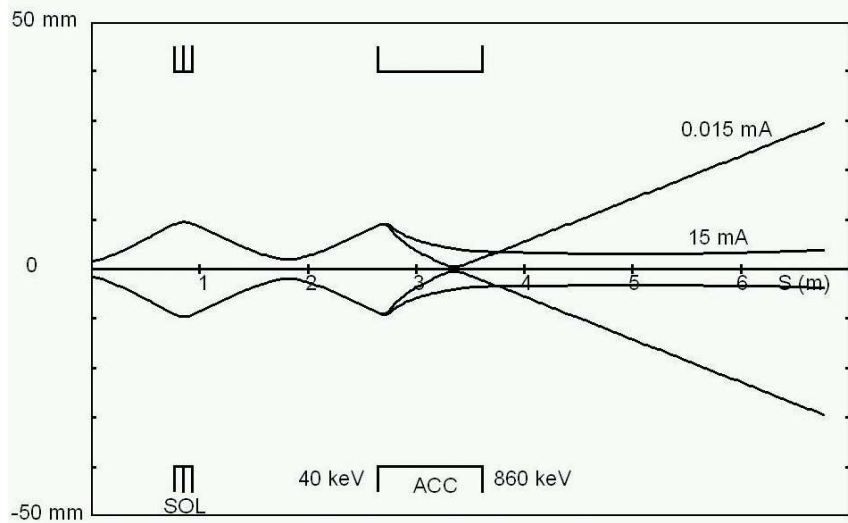


Fig. 13: Envelopes of a low- and high-current proton beam calculated with the PSI Graphic Transport Framework of U. Rohrer [13]. SOL: Solenoid, ACC: Accelerator tube, acceleration from 40 to 860 keV. The electric field transition at the entrance of the tube yields a strong focusing effect. The low-current beam exhibits a narrow waist inside the tube. The high-current beam is defocused by the space charge forces inside the tube yielding a weak waist at a distance of 1.4 m from the accelerator exit. Outside the tube the space charge forces are neutralized. The emittance at 40 keV is $20 \pi \text{ mm mrad}$.

The example shows the beam envelope in the region an electrostatic accelerator tube. It is a Cockcroft–Walton accelerator which is used as preaccelerator for the PSI injector cyclotron. In this example a high-current proton beam (15 mA) with an energy of 40 keV leaves the ion source. For comparison, the envelopes of a low current beam (0.015 mA) are also shown. A solenoid is used to refocus the beam yielding a waist between the solenoid and the accelerator tube. The 1 m long acceleration tube accelerates the beam to a kinetic energy of 860 keV. The voltage gradient inside the acceleration tube is constant. The focusing effect of the electric field transition at the entrance of the tube can be clearly seen. The defocusing effect at the exit of the acceleration tube is so weak that it cannot be seen.

Outside the acceleration tube the positive charge of the beam particles is assumed to be neutralized by negatively charged particles (secondary electrons from the residual gas of the vacuum). There is no neutralization of the space charge forces inside the tube. The space charge forces inside the tube have been taken into account by adding a series of thin defocusing lenses. This can be easily realized by using the element ‘Space Charge’ of the PSI Transport program [13]. As a consequence the envelope of the high-current beam is modified such that a broad waist appears outside of the acceleration tube. In contrast to that the low-current beam exhibits a narrow waist inside the accelerator tube. The example shows that space charge forces can have a strong influence on the ion optics.

11 Conclusion

The ion optics of electrostatic lenses is presented. The first-order transport matrices are derived for the accelerating tube lens, the aperture lens, the einzel lens, the electrostatic quadrupole and the electrostatic deflector. The structure of telescopic systems is sketched. The analogy with geometrical optics is discussed. Phase ellipses and beam envelopes are described using the so-called σ matrices. The effect of space charge forces is discussed and a numerical example using the PSI Graphic Transport program is shown.

Acknowledgements

I would like to thank Håkan Danared, Dag Reistad, Vasily Parkhomchouk, Urs Rohrer and Volker Ziemann for helpful informations and discussions. I would especially like to thank Urs Rohrer for his advice and help in using the PSI Graphic Transport program.

Copyright notice

Figures 1–9 are reprinted from F. Hinterberger, *Physik der Teilchenbeschleuniger und Ionenoptik*, Springer-Verlag Berlin Heidelberg New York 1997, Chapter 4 and 5 with kind permission of Springer Science and Business Media (copyright 2005).

References

- [1] R. Gans, *Z. Tech. Phys.* **18** (1937) 41.
- [2] M. Elkind, *Rev. Sci. Instrum.* **24** (1953) 129.
- [3] U. Timm, *Z. Naturforsch.* **10a** (1955) 593.
- [4] A. Galejs and P.H. Rose, Optics of electrostatic accelerator tubes, in *Focusing of Charged Particles*, vol. II, ed. A. Septier (Academic Press, New York, 1967).
- [5] V.K. Zworykin, G.A. Morton, E.G. Ramberg, J. Hillier, A.W. Vance, *Electron Optics and the Electron Microscope* (Wiley, New York, 1945).
- [6] J.D. Lawson, *The Physics of Charged Particle Beams* (Clarendon Press, Oxford, 1988).
- [7] F. Hinterberger, *Physik der Teilchenbeschleuniger und Ionenoptik* (Springer-Verlag, Berlin, 1997).
- [8] A.P. Banford, *The Transport of Charged Beams* (E. & F. N. Spon, London, 1966).
- [9] P. Dahl, *Introduction to Electron and Ion Optics* (Academic Press, New York, 1973).
- [10] H. Wollnik, *Optics of Charged Particles* (Academic Press, Orlando, 1987).
- [11] K.L. Brown, D.C. Carey, Ch. Iselin and F. Rothacker, CERN Report 80-04 (1980).
- [12] D.C. Carey, The optics of charged particle beams, in *Accelerators and Storage Rings* **6** (1987) 1–289, eds. Blewett, J.P. and Cole, F.T. (Harwood, Chur, 1987).
- [13] U. Rohrer, About Graphic Transport, PSI Note (2005), http://people.web.psi.ch/rohrer_u/trans.htm, based on a CERN-SLAC-FERMILAB version by K.L. Brown, D.C. Carey, Ch. Iselin and F. Rothacker, CERN Report 80-04 (1980).
- [14] Figure reprinted from F. Hinterberger, *Physik der Teilchenbeschleuniger und Ionenoptik*, Springer-Verlag Berlin, 1997, Chapters 4 and 5, with kind permission of Springer Science and Business Media (copyright 2005).
- [15] F. Ollendorff, *Elektronik des Einzelelektrons* (Springer-Verlag, Vienna, 1955).
- [16] F. Hinterberger, *Nucl. Instrum. Methods* **111** (1973) 189.
- [17] K.L. Brown, *IEEE Trans. Nucl. Sci.* **NS-26** (1979) 3490.
- [18] C.M. Merry and J.C. Cornell, *SA J. Phys.* **6** (1983) 12.
- [19] F.J. Sacherer, *IEEE Trans. Nucl Sci.* **NS-18** (1971) 1105.
- [20] F.J. Sacherer and T.R. Sherwood, *IEEE Trans. Nucl Sci.* **NS-18** (1971) 1066.